APPENDIX H

FRACTURE PROPERTIES OF ASPHALT MIXTURES

LIST OF FIGURES

LIST OF TABLES

The equations of the fracture properties to calculate the Paris's law coefficients A, n and a_k are:

$$\log A = g_2 + \frac{g_3}{m_{mix}} \log D_1 + g_4 \log \sigma_t \qquad \text{(H-1)}$$

$$n = g_0 + \frac{g_1}{m_{mix}} \qquad \text{(H-2)}$$

$$a_k = \int_0^{\Delta t} w(t)^n \, dt \qquad \text{(H-3)}$$

where $g_0, g_1, g_2, g_3,$ and g_4 are the fatigue calibration coefficients;

m_{mix} is the slope of the graph of the relaxation modulus (E_i) vs loading time (t_i);

D_1 is the coefficient in the master creep compliance power law equation;

σ_t is undamaged tensile strength;

$w(t)$ is the normalized load wave shape for different axles and thermal loading.

The fatigue calibration coefficients $g_0, g_1, g_2, g_3,$ and g_4 were developed in the SHRP A-003A project and reported in the SHRP Report A-357 (4). These coefficients are shown in Table H-1 in all four climate zones. The variable m_{mix} is the slope of the graph of the ANN relaxation modulus (E_i) versus the loading time (t_i). The three thermal loading times are based on the time during which the temperature is below the stress free temperature (20°C) as illustrated in Figure H-1. These times are used to calculate the m_{mix} for the thermal case Figure H-2. On the other hand, the traffic loading time was determined by the eight axle categories shown in Figure H-3. Since the variance of pavement temperature could be significant, it was necessary to calculate the m_{mix} hourly.

Table H-1. Tensile strength of asphalt mixtures.

	Tensile Strength (psi)	Temperature (°F)	r (in/m in)
Thermal	$\sigma_t = \left[\frac{E(t,T)(MPa)}{21.3} \right]^{\frac{1}{1.95}}$	77	0.005
Traffic	$\sigma_t = \left[\frac{E(t,T)(MPa)}{45.5} \right]^{\frac{1}{1.56}}$	77	0.5

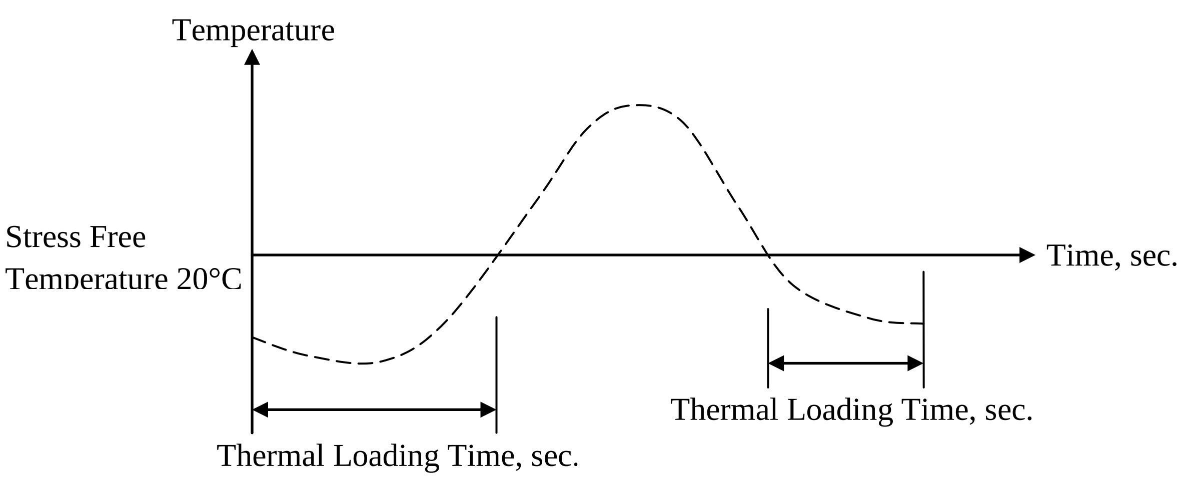

Figure H-1. Loading time under stress free temperature.

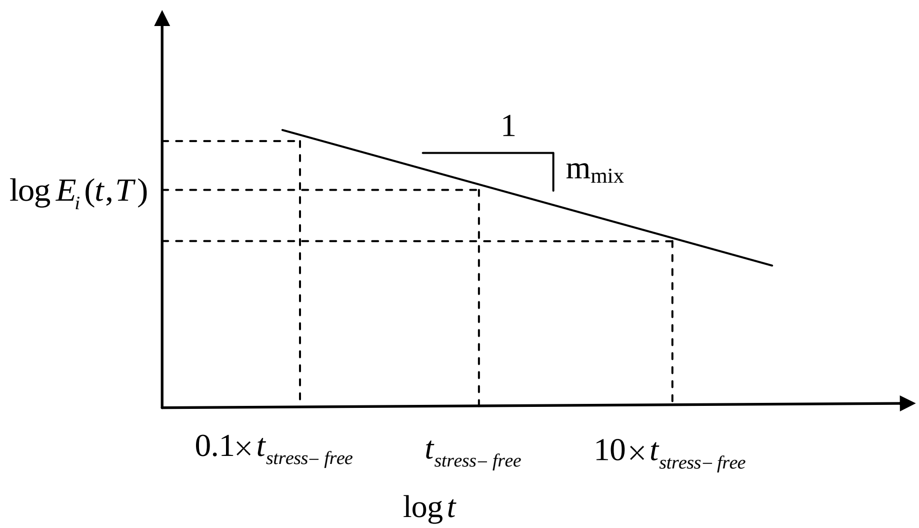

Figure H-2. Method to evaluate the m_{mix} of fracture properties for thermal case.

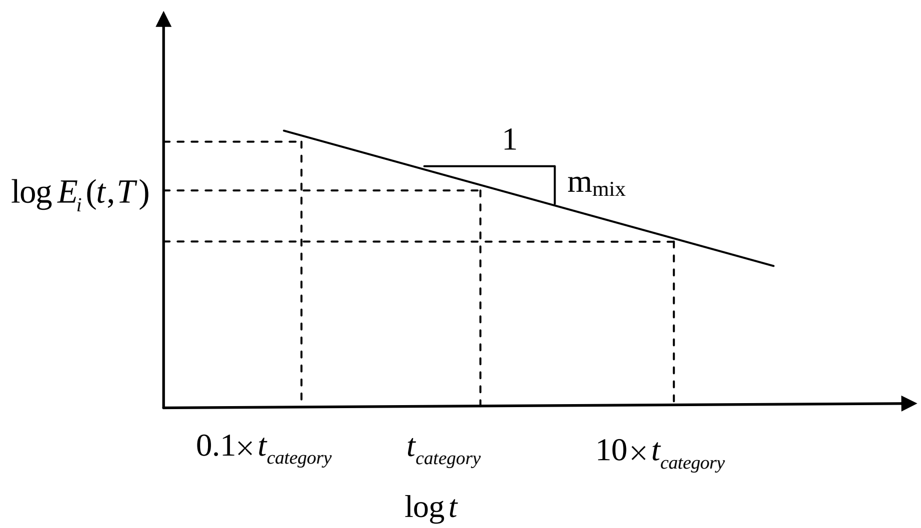

Figure H-3. Method to evaluate the m_{mix} of fracture properties for traffic case.

The other unknown term is tensile strength σ_t . The equations of tensile strength σ_t are different in thermal and traffic cases shown in Table H-1.

The coefficient D_1 is the coefficient in the master creep compliance power law equation which is shown in (H-4). In the Calibration program, E_1 is calculated by Equation (H-5). For the design program, the equation for E_1 is Equation (H-6) which is not a function of the FWD modulus.

$$D_1 = \frac{\sin(m_{mix} \times \pi)}{E_1 \times m_{mix} \times \pi} (psi) \tag{H-4}$$

$$\log E_1(t,T) = \log E_{ANN}(\frac{t_{FWD}}{a_T}, T) - m_{mix-FWD} \times \log(\frac{t_{FWD}}{a_T}) \tag{H-5}$$

$$\log E_1(t,T) = \log E(t,T) - m_{mix} \times \log(\frac{t}{a_T}) \tag{H-6}$$

where $m_{mix-FWD}$ is the slope of the graph of the ANN relaxation moduli versus loading time; a_T is the shift factor based on the FWD temperature (T_{FWD}) (H-7), C_1, C_2, and T_d are the parameters of the Time- Temperature shift function in Table H-2;

$$a_T = 10^{\frac{-C_1(T_{FWD} - T_d)}{C_2 + T_{FWD} - T_d}} \tag{H-7}$$

The method to obtain the $m_{mix-FWD}$ is basically the same as m_{mix} that we introduced earlier in Figure H-4. Assuming the FWD loading time is 0.06 second, consider three loading times which are FWD loading time divided by shift factor, 10 times the FWD loading time divided by the shift factor, and 0.1 times the FWD loading time divided by the shift factor. Use these loading times and the FWD testing temperature to evaluate the relaxation moduli, and find the $m_{mix-FWD}$.

Table H-2. Fatigue calibration coefficients for four climate zones.

	Wet-Freeze	Wet-No Freeze	Dry-Freeze	Dry-No Freeze
g_0	-2.09	-1.429	-2.121	-2.024
g_1	1.952	1.971	1.677	1.952
g_2	-6.108	-6.174	-5.937	-6.107
g_3	0.154	0.19	0.192	1.53
g_4	-2.111	-2.079	-2.048	-2.113
g_5	0.037	0.128	0.071	0.057
g_6	0.261	1.075	0.762	0.492
T_d (°C)	-5.8	-6.4125	-6.22	-6.07142857
C_1	31.57	42.49	38.77	41.55
C_2	199.21	259.28	239.04	266.89

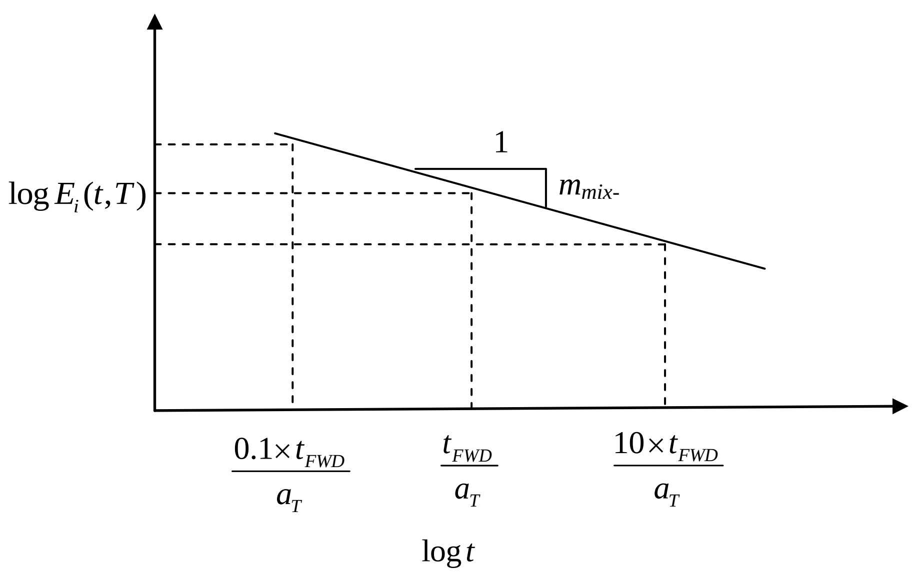

Figure H-4. Method to evaluate the $m_{mix-FWD}$.

The healing coefficients g_5 and g_6 are used in defining the healing shift factor which is based on the average time between passing vehicles, Δt. The healing shift factor is

$$SF_{healing} = 1 + g_5 \left(\Delta t\right)^{g_6} \tag{H-8}$$

The healing shift factor divides into each day's traffic crack growth and thus prolongs the number of days required for the crack to reach the surface of the overlay.

Fracture property a_k is a traffic factor which is a function of the load wave shape $w(t)$ (H-3). Since the load wave shapes are different for different axle combinations, therefore, we considered single axle, tandem axle, tridem axle, and quadrem axle in both the bending and shearing cases in this program for the traffic loading, and set $a_k = 1$ for the thermal case. In order to evaluate the a_k, the load wave shape for different axles was determined, and then the load wave shape raised to the power *n* was integrated between the time limits of zero and Δt. The equations of Δt for different axles are shown in Table H-3. L_j is the length of the tire footprint, *V* is the speed of travel (H-9), and *n* is the Paris's law coefficient (H-2). Figures H-5 to H-12 are the load wave shapes for different axles in the bending and shearing cases.

$$a_k = \int_0^{\Delta t} w(t)^n \, dt$$

$$\text{Speed of Travel}, V = V \frac{miles}{hour} \times \frac{22 \frac{ft}{\text{sec.}}}{15 \frac{miles}{hour}} \tag{H-9}$$

Table H-3. Upper limit of integration of a_k in different axles.

	Δt (second)
Single Axle	$\frac{L_j + 10\, ft}{V}$
Tandem Axle	$\frac{L_j + 14\, ft}{V}$
Tridem Axle	$\frac{L_j + 18\, ft}{V}$
Quadrem Axle	$\frac{L_j + 22\, ft}{V}$

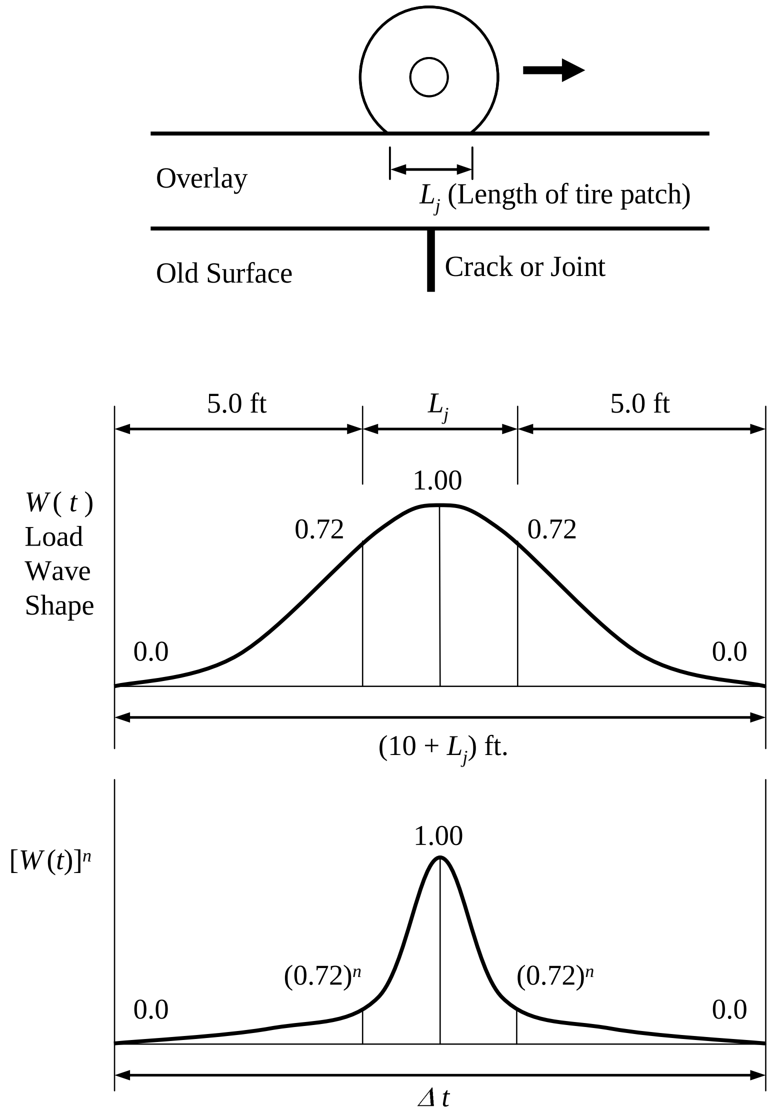

Figure H-5. Load wave shape for single axle in bending crack propagation.

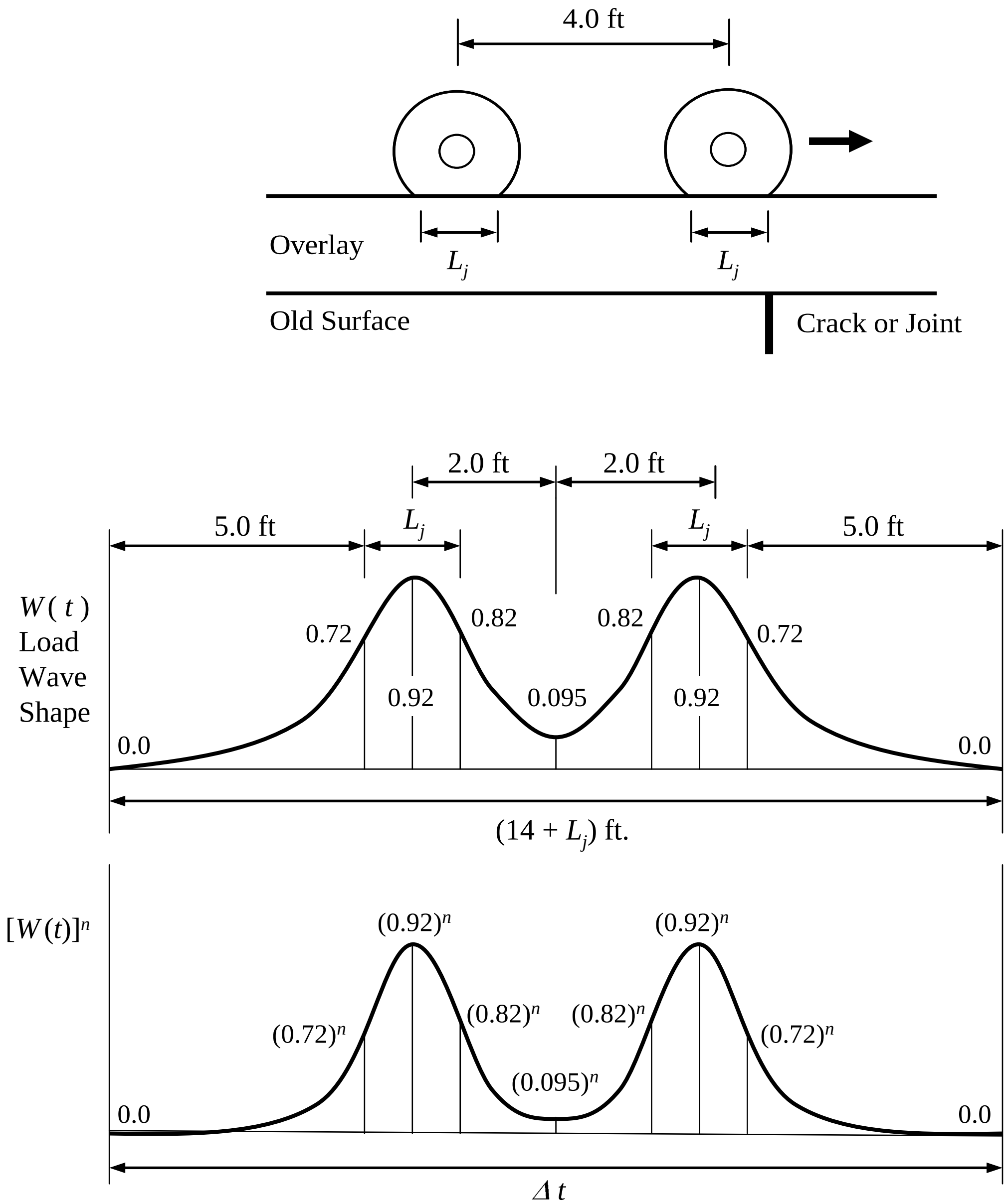

Figure H-6. Load wave shape for tandem axle in bending crack propagation.

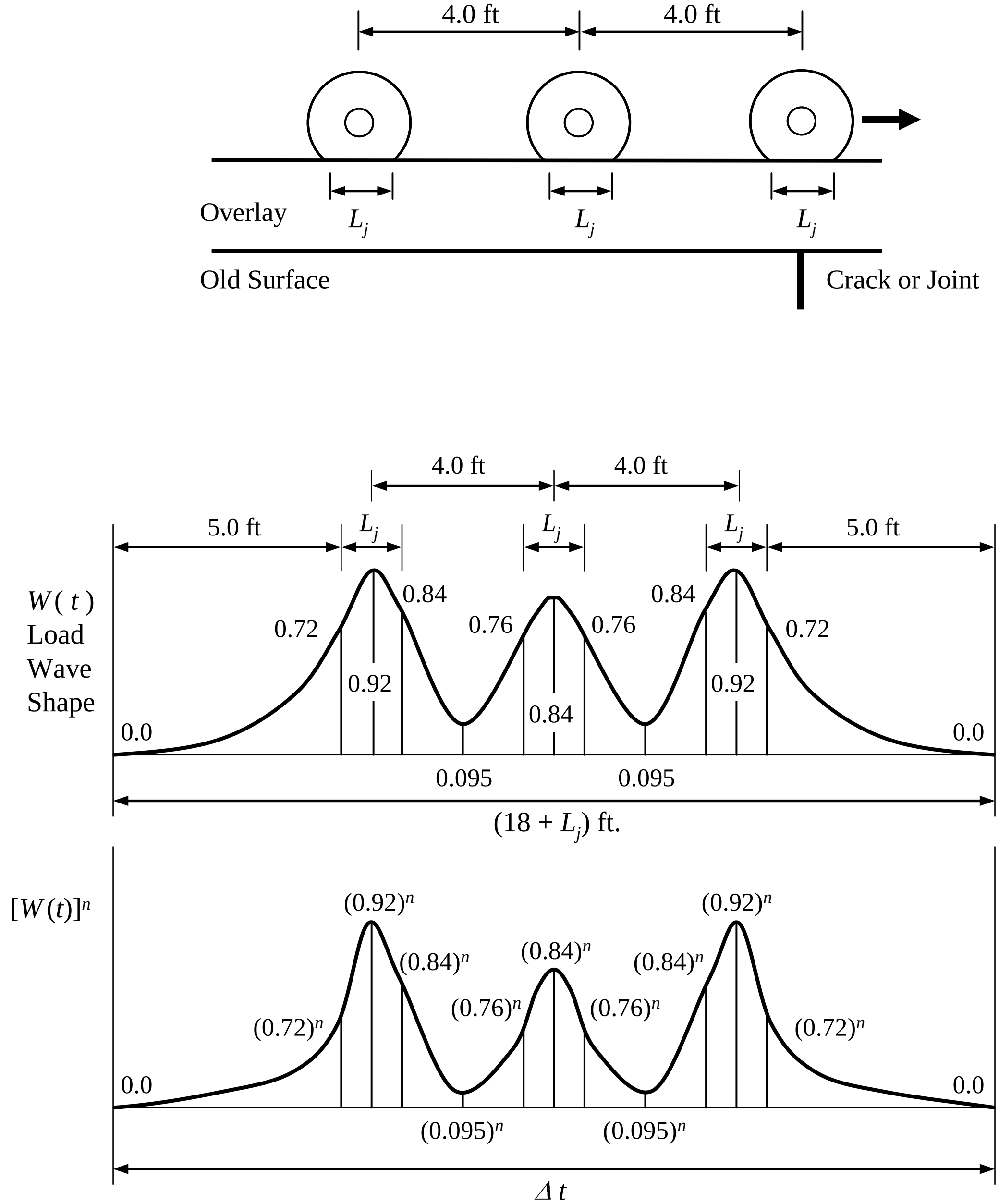

Figure H-7. Load wave shape for triple axle in bending crack propagation.

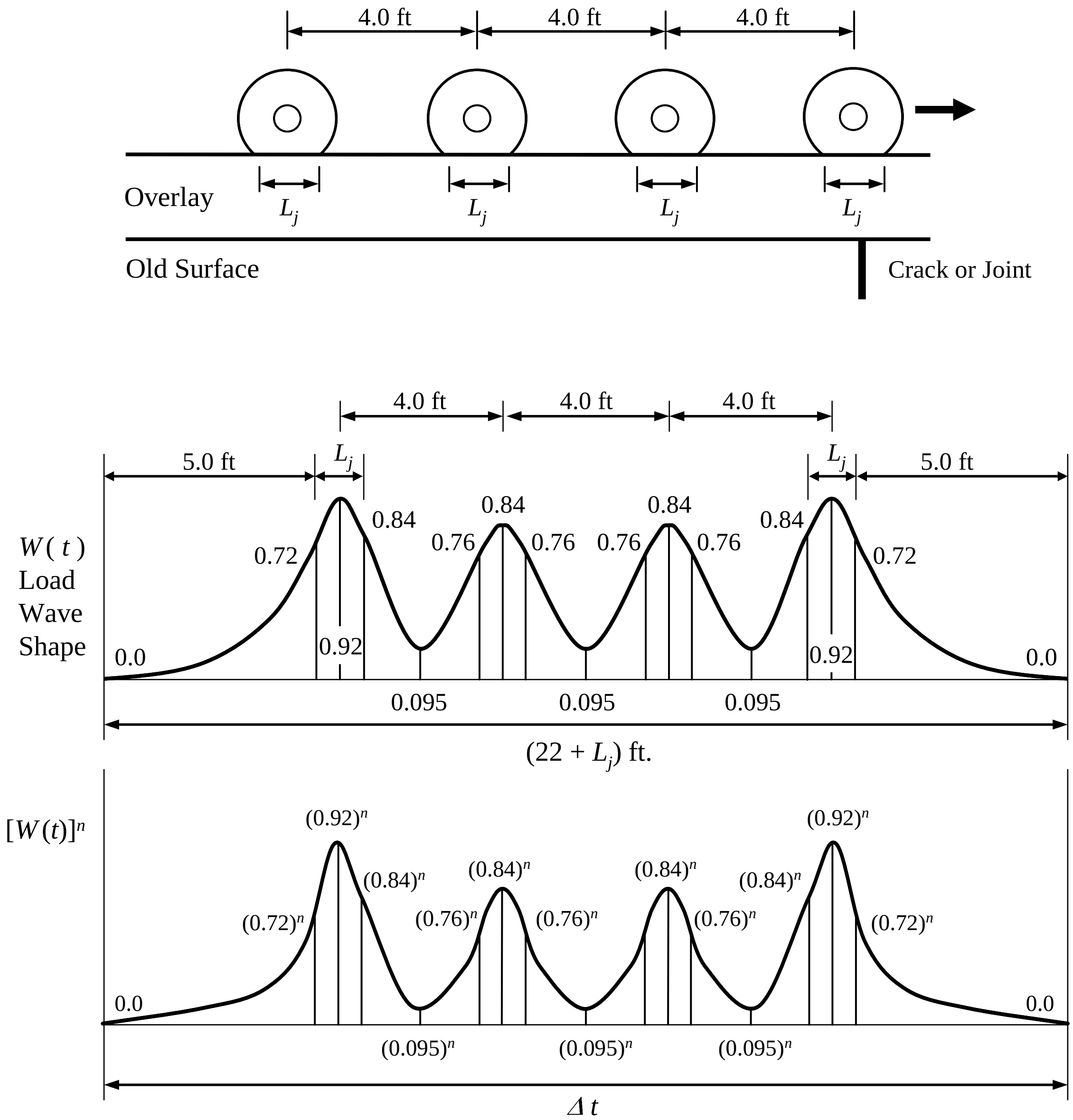

Figure H-8. Load wave shape for quad axle in bending crack propagation.

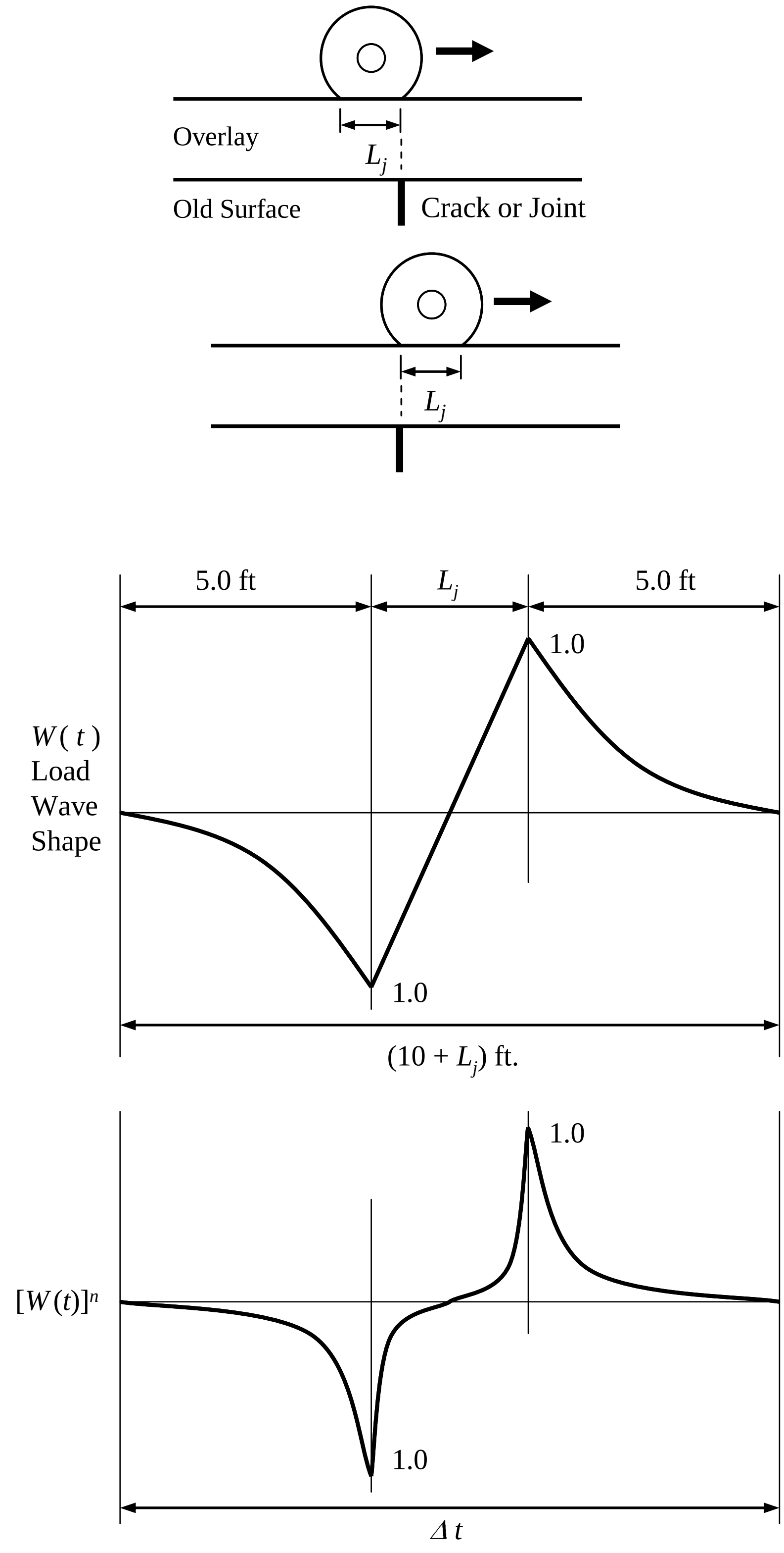

Figure H-9. Load wave shape for single axle in shearing crack propagation.

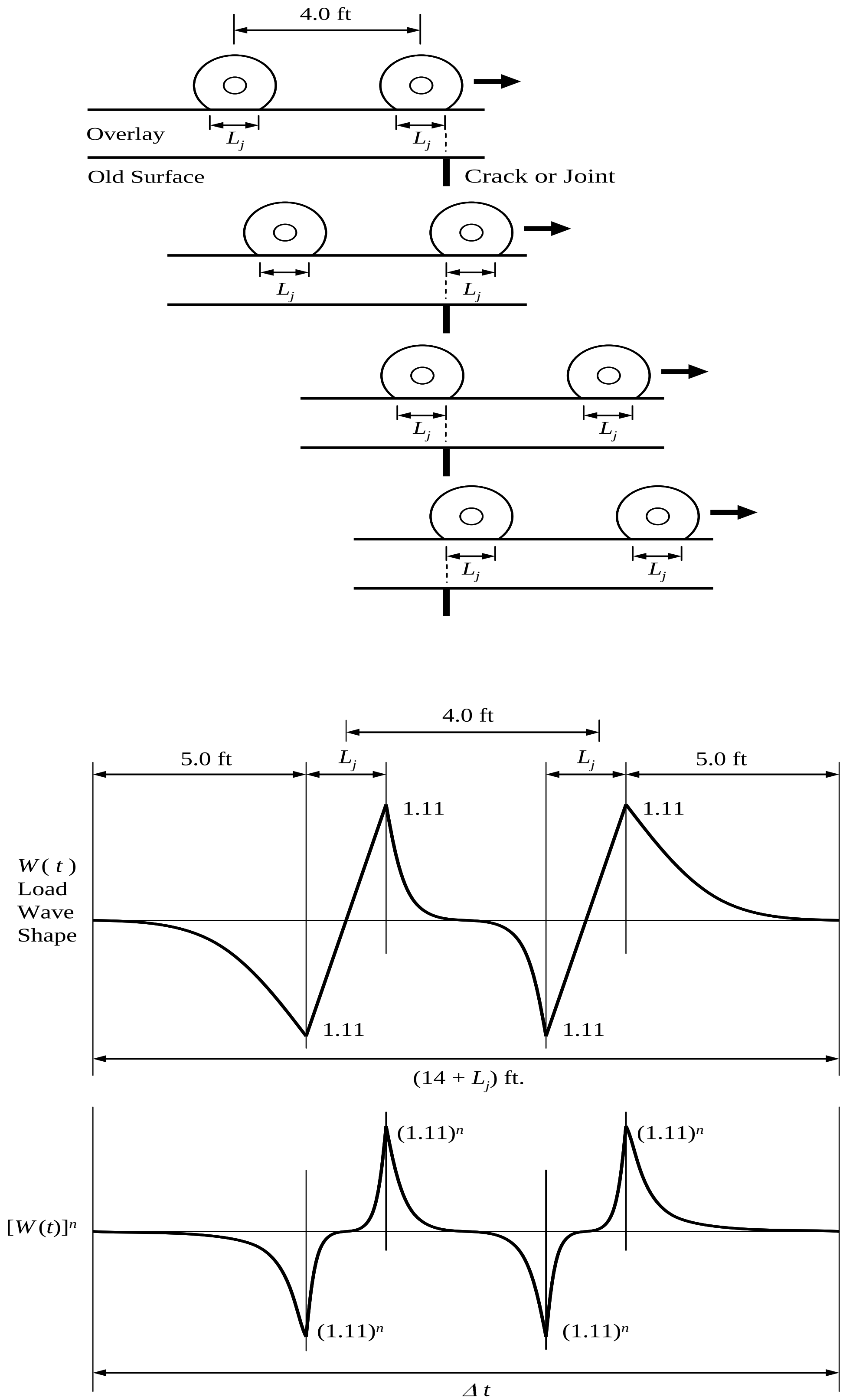

Figure H-10. Load wave shape for tandem axle in shearing crack propagation.

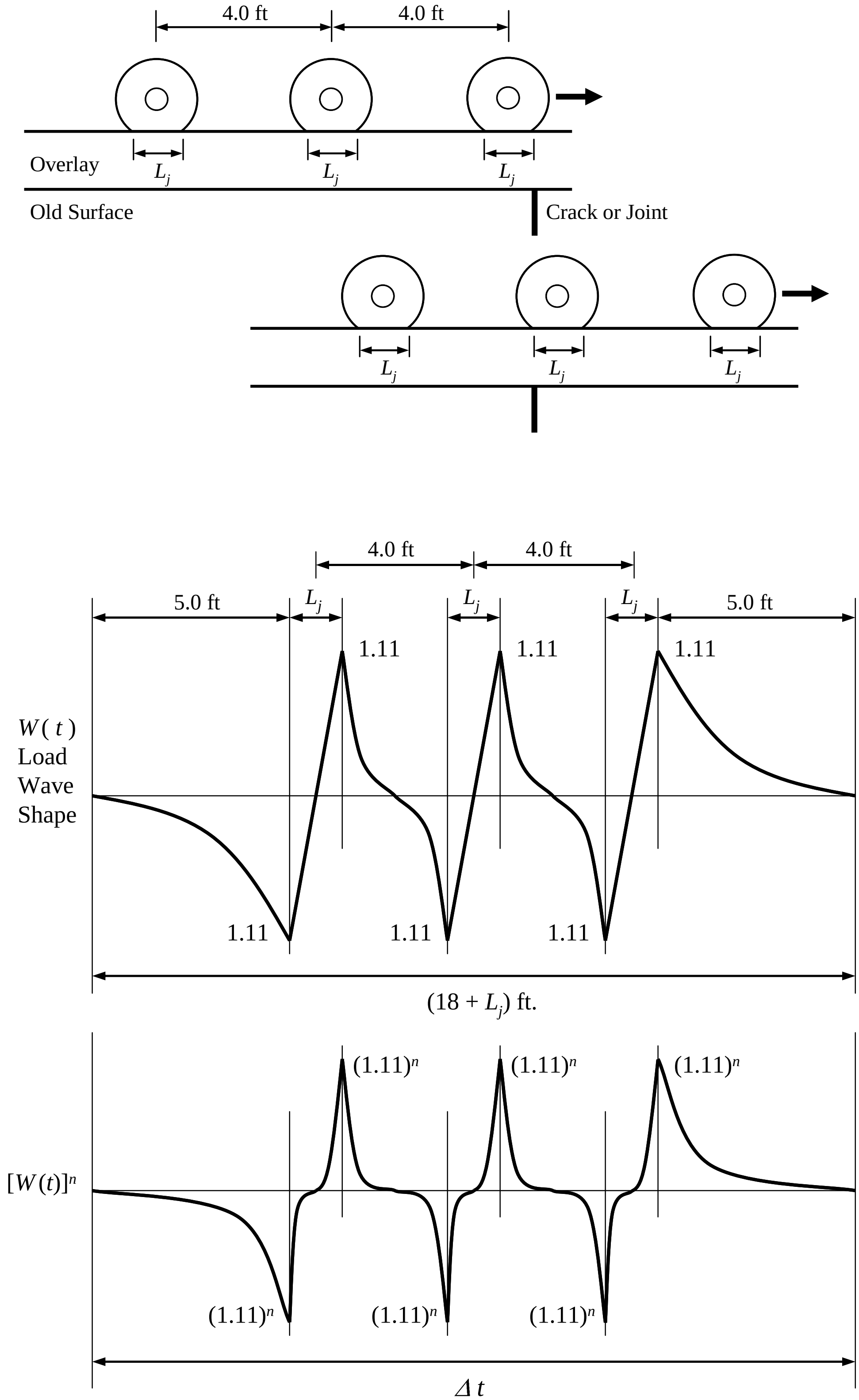

Figure H-11. Load wave shape for triple axle in shearing crack propagation.

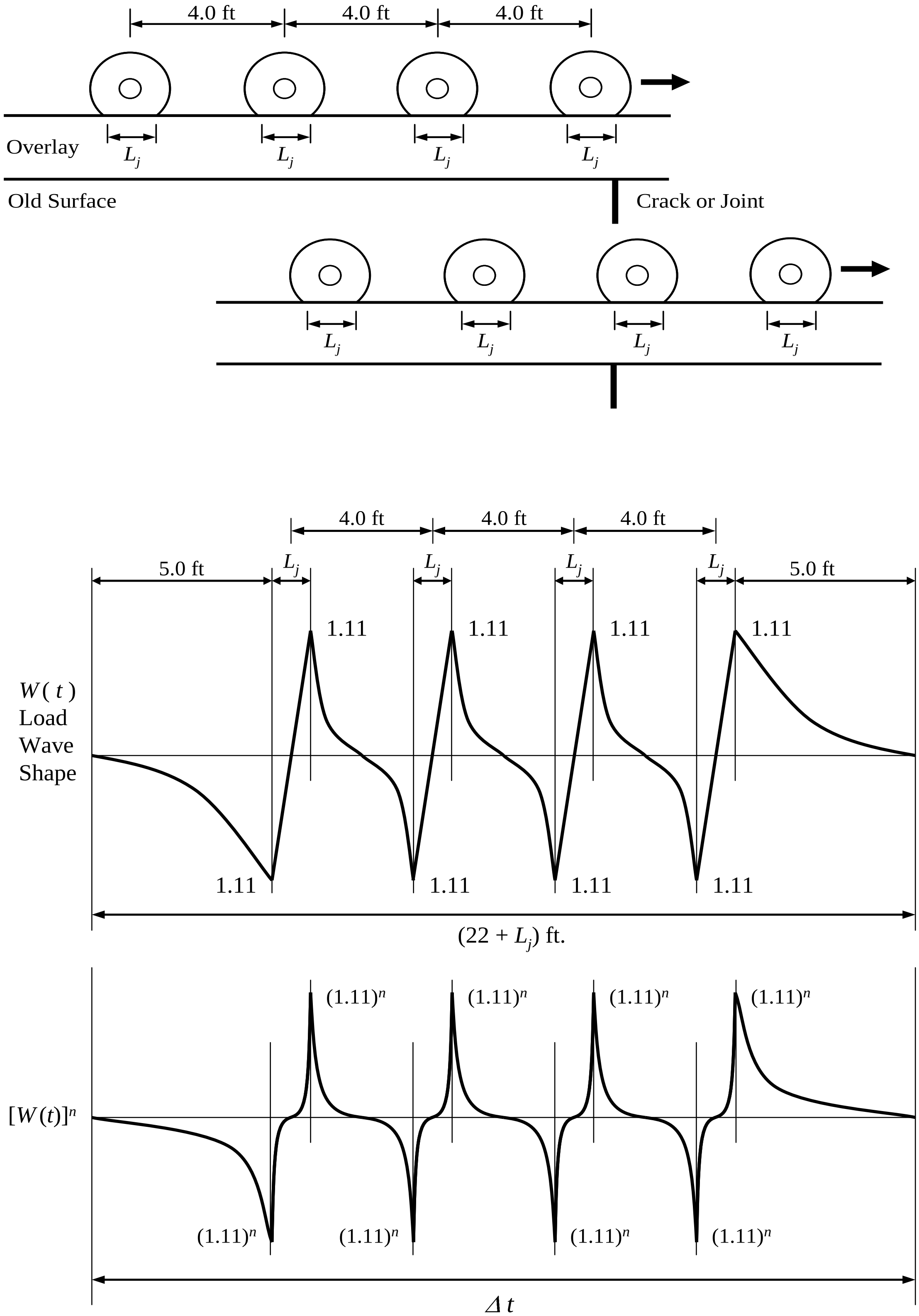

Figure H-12. Load wave shape for quad axle in shearing crack propagation.